Acta Pharmaceutica Sinica B 2024;14(10):4396–4412

Chinese Pharmaceutical Association
Institute of Materia Medica, Chinese Academy of Medical Sciences

Acta Pharmaceutica Sinica B

www.elsevier.com/locate/apsb
www.sciencedirect.com

ORIGINAL ARTICLE

# Reprogramming tumor-associated macrophages and inhibiting tumor neovascularization by targeting MANF–HSF1–HSP70-1 pathway: An effective treatment for hepatocellular carcinoma

**Dan Han [a,b,†], Qiannan Ma [a,b,†], Petek Ballar [c], Chunyang Zhang [a,b], Min Dai [a,b], Xiaoyuan Luo [a,b], Jiong Gu [d], Chuansheng Wei [a,b], Panhui Guo [e], Lulu Zeng [e], Min Hu [e], Can Jiang [a,b], Yanyan Liang [a,b], Yanyan Wang [a,b], Chao Hou [a], Xian Wang [a], Lijie Feng [a,b], Yujun Shen [a,b], Yuxian Shen [a,b,*], Xiangpeng Hu [e,*], Jun Liu [a,b,*]**

[a]*School of Basic Medical Sciences, Anhui Medical University, Hefei 230032, China*
[b]*Biopharmaceutical Research Institute, Anhui Medical University, Hefei 230032, China*
[c]*Department of Biochemistry, Faculty of Pharmacy, Ege University, Izmir 35130, Turkey*
[d]*Department of General Surgery, the Second Affiliated Hospital of Anhui Medical University, Hefei 230061, China*
[e]*Department of Gastroenterology, the Second Affiliated Hospital of Anhui Medical University, Hefei 230061, China*

Received 26 January 2024; received in revised form 9 April 2024; accepted 26 April 2024

**KEY WORDS**

Mesencephalic astrocyte-derived neurotrophic factor;
Neovascularization;
Hepatocellular carcinoma;

**Abstract** In advanced hepatocellular carcinoma (HCC) tissues, M2-like tumor-associated macrophages (TAMs) are in the majority and promotes HCC progression. Contrary to the pro-tumor effect of M2-like TAMs, M1-like TAMs account for a small proportion and have anti-tumor effects. Since TAMs can switch from one type to another, reprogramming TAMs may be an important treatment for HCC therapy. However, the mechanisms of phenotypic switch and reprogramming TAMs are still obscure. In this study, we analyzed differential genes in normal macrophages and TAMs, and found that loss of MANF in TAMs

*Corresponding authors.
E-mail addresses: shenyx@ahmu.edu.cn (Yuxian Shen), xphuay2003@aliyun.com (Xiangpeng Hu), liujun@ahmu.edu.cn (Jun Liu).
[†]These authors made equal contributions to this work.
Peer review under the responsibility of Chinese Pharmaceutical Association and Institute of Materia Medica, Chinese Academy of Medical Sciences.

https://doi.org/10.1016/j.apsb.2024.05.001

Reprogramming tumor-associated macrophages;
Monocyte-derived hepatic macrophage

accompanied by high levels of downstream genes negatively regulated by MANF. MANF reprogrammed TAMs into M1 phenotype. Meanwhile, loss of MANF promoted HCC progression in HCC patients and mice HCC model, especially tumor neovascularization. Additionally, macrophages with MANF supplement suppressed HCC progression in mice, suggesting MANF supplement in macrophage was an effective treatment for HCC. Mechanistically, MANF enhanced the HSF1−HSP70-1 interaction, restricted HSF1 in the cytoplasm of macrophages, and decreased both mRNA and protein levels of HSP70-1, which in turn led to reprogramming TAMs, and suppressing neovascularization of HCC. Our study contributes to the exploration the mechanism of TAMs reprogramming, which may provide insights for future therapeutic exploitation of HCC neovascularization.



## 1. Introduction

Hepatocellular carcinoma (HCC) is the most common type of primary liver cancer and one of the leading causes of cancer death worldwide[1,2]. It is predicted that the number of HCC patients is more than one million by 2025[3]. Commonly used treatments of HCC include surgery, radiation therapy, chemotherapy, immunotherapy and targeted drug therapy[4]. Despite a variety of HCC treatments, advanced stage HCC remains incorrigible because of cancer recurrence, therapeutic resistance and low response to immunotherapy[5-7]. Therefore, the therapy effect and prognosis are not satisfactory, and HCC treatment remains a global challenge.

Macrophages in tumor tissues are called tumor-associated macrophages (TAMs)[8], which are one of the main members in the HCC microenvironment[9]. In advanced cancer tissues, M2-like TAMs are in the majority[10], and play an important role in the progression of HCC, including promoting immunosuppression, neovascularization, the proliferation and metastasis of hepatomas[9]. Contrary to the pro-tumor effect of M2-like TAMs, M1-like TAMs account for a small proportion and have anti-tumor effects[10]. Since TAMs can switch from one type to another[11], reprogramming TAMs is used to defeat cancer tissues[12]. However, the mechanisms of phenotypic switch of TAMs and reprogramming TAMs are still obscure.

In the current study, we analyzed differential genes in normal macrophages (NMs) and TAMs, and found that loss of MANF in TAMs accompanied by high levels of downstream genes negatively regulated by MANF. Meanwhile, loss of MANF in macrophages led to the M2-like phenotype and promoted HCC neovascularization. Mechanistically, MANF stabilized the interaction of heat shock factor 1 (HSF1) and heat shock protein 70-1 (HSP70-1), inhibited HSF1 nuclear import, suppressed the transcriptional activity of HSF1 and reduced HSP70-1 level. Additionally, we verified that MANF supplement in macrophages was an effective therapy for HCC in mice orthotopic implantation HCC model. Our study contributes to the exploration the mechanism of TAMs reprogramming, which may provide insights for future therapeutic exploitation of HCC neovascularization.

## 2. Materials and methods

### 2.1. Human samples and ethics statement

The human samples were collected from the Second Affiliated Hospital of Anhui Medical University and the informed consents were obtained before enrolling participants in this study. Blood samples of HCC patients in General Surgery Department were collected before any treatment, and control blood samples were taken from the Hospital Health Examination Center. Liver tissues of HCC patients were obtained from tissues discarded after surgery. The exclusion criteria for healthy volunteers are abnormal physical examination, and the exclusion criteria for HCC patients are that patients received therapy before surgery. At last, 21 healthy volunteers and 24 HCC patients are included in this research. The use of clinical HCC specimens was in line with the Declaration of Helsinki. This study was approved by the Ethics Committee of Anhui Medical University (No. 20200839).

### 2.2. Human HCC organoid culture and collection of organoid culture medium

Human liver cancer tissues were collected, digested with Collagenase IV and DNase I, and terminated digestion with AdDMEM/F12. The isolated cells were filtered by 70 μm filter, washed with AdDMEM/F12, and mixed with Matrigel in low adhesion plates. After the plates were incubated at 37 °C for 30 min, the culture supernatant was added into the plates according to the protocol[13]. The details of reagents were described in the supporting Information. Two weeks later, the organoids were harvested, passaged at the density of 1:3, re-mixed with Matrigel for culture. The organoid culture medium was changed every 3 days, and the discarded culture medium was collected and aliquoted, which was stored at −80 °C.

### 2.3. Orthotopic transplantation of mice HCC model

Eight-week-old male C57BL/6J mice were purchased from Gempharmatech (Nanjing, China) for the experiment of orthotopic implantation HCC model. For the orthotopic tumor model, Hep1-6-Luc cells were mixed with Matrigel Matrix and injected into left lobe liver ($5 \times 10^6$ cells/mouse) under 2%−3% isoflurane anesthesia. Seven days following orthotopic tumor implantation, RAW264.7 cells ($1 \times 10^6$ cells/mouse) treated with recombination MANF protein were injected through the tail vein every 2 days, and sorafenib (5 mg/kg) was injected as a positive control drug. *In vivo* imaging was performed, and mice were harvested at 18 days after tumor implantation. All the mice experiments were approved by the Animal Experimental Committee of Anhui Medical University (No. LLSC20200827).

### 2.4. DEN-induced liver spontaneous mice HCC model

$MANF^{flox/flox}$ mice were described in our previous study[14], which were cross-bred with Lyz2-cre mice (RRID: IMSR_JAX: 018956) or Alb-cre mice (RRID: IMSR_JAX: 003574) to specifically knock out the *Manf* gene in myeloid lineage cells (MANF-MKO [knockout] mice) or in hepatocytes (HKO [knockout] mice). The details of *N*-nitrosodiethylamine (DEN)-induced HCC mouse model were described in our previous study[14]. All the mice experiments were approved by the Animal Experimental Committee of Anhui Medical University (No. LLSC20200827).

### 2.5. Cell lines

THP-1, U937, HEK 293T, and HUVEC cells were obtained from the American Type Culture Collection and cultured according to the instructions. THP-1 and U937 cells were cultured with RPMI-1640 containing 10% fetal bovine serum. PMA (100 ng/mL) was used to treat THP-1 and U937 cells for 24 h to polarize into macrophages. HEK 293T cells were cultured with DMEM/high glucose containing 10% fetal bovine serum. HUVEC cells were cultured with Endothelial Cell Medium (ScienCell).

### 2.6. Antibodies, reagents and plasmids

The details of antibodies, reagents and plasmids are described in the Supporting Information.

### 2.7. Cells transfection for knockdown and overexpression of MANF

The sequence of *MANF*-siRNA used to knockdown the *MANF* gene in THP-1 cells or U937 cells is as follows: Forward: 5′-GGCAAAGAGAAUCGGUUGUTT-3′; Reverse: 5′-ACAA CCGAUUCUCUUUGCCTT-3′. Advanced transfected reagent (ZETA Life, CA, USA) was used to transfect THP-1 cell and U937 cells according to the manufacturer's protocol. 293T cells were transfected with pLVML-3 × FLAG-*MANF*-MCS-Puro, pMD2G and psPAX2 plasmids in 6-well-plate. Twenty-four hours later, the medium of 293T cells was collected, and then used to transfect THP-1 or U937 cells to overexpress MANF protein. Lipo3000 was used to transfected with GFP-MANF plasmid in THP-1 or U937 cells according to the protocol provided by manufacturer.

### 2.8. Immunohistochemistry and integral of optical density (IOD), double-labelling immunofluorescence, hematoxylin-eosin (HE) staining, Western blot assay, quantitative real-time polymerase chain reaction (qPCR), MTT assay, co-immunoprecipitation (Co-IP), extraction of cytoplasmic and nuclear proteins

The details of these experiment methods were described in our previous study[14,15], and the primer sequences for QPCR assays are presented in the Supporting Information.

### 2.9. Isolation of mice primary hepatocytes and hepatic macrophages, TUNEL assay, extraction of human peripheral blood monocytes (PBMs), tube formation assay in vitro, extraction and purification of recombinant MANF protein, GST pull-down

The details of these experimental methods are described in the Supporting Information.

### 2.10. RNA sequencing of primary macrophages from MANF deficiency mice

The primary peritoneal macrophages were extracted from MKO mice and control WT mice for RNA sequencing, and RNA sequencing was performed by Oebiotech Corporation (Shanghai, China). The sequence data were uploaded to NCBI Sequence Read Archive (SRA) under the accession number PRJNA921728.

### 2.11. RNA sequencing analysis of different genes expression between normal macrophage and TAMs

The RNA sequencing[16] was downloading from GEO database (GSE158792). PMA (100 ng/mL) was used to treat THP-1 cells for 24 h in order to promote the polarization into macrophages, and the PMA-treated macrophages were normal macrophages (NMs). Meanwhile, PMA-treated THP-1 cells that were co-cultured with HepG2 for 48 h were TAMs. The differentially expressed genes were analyzed between NMs and TAMs.

### 2.12. Statistical analysis

One-way ANOVA was used to analyze the difference between various expressions in HKO, MKO and WT mice. Independent-Sample *T* test was used to analyze the difference of 2 groups. Spearman correlation analysis was used to detect the relationship of PBMs-derived MANF level and CD31 level in the liver cancer tissues. All the date are expressed as mean ± standard deviation (SD). $P < 0.05$ were considered statistically significant.

## 3. Results

### 3.1. MANF reprograms TAMs into M1-like phenotype

The RNA sequencing[16] was analyzed. We found the level of *MANF* was statistically significant decreased (Fig. 1A and B) and the levels of downstream genes negatively regulated by MANF at the transcription level were increased (Fig. 1B) in TAMs, compared with those in NMs. We also found that there was no difference of *Snail2* between NMs and TAMs (Fig. 1B), which was a downstream molecular negatively regulated by MANF at protein level[14]. The data suggested that MANF might be an important regulator of TAMs. Then, we detected the level of hepatic macrophage-derived MANF in cancer tissues and para-cancer tissues of HCC patient and DEN-induced mice HCC model. These data showed that MANF was decreased in the hepatic macrophages of cancer tissues, compared to that in para-cancer tissues (Supporting Information Fig. S1A–S1H). Next, PMA-treated THP-1 cells were transfected with MANF-siRNA to knockdown MANF, and the results indicated that MANF

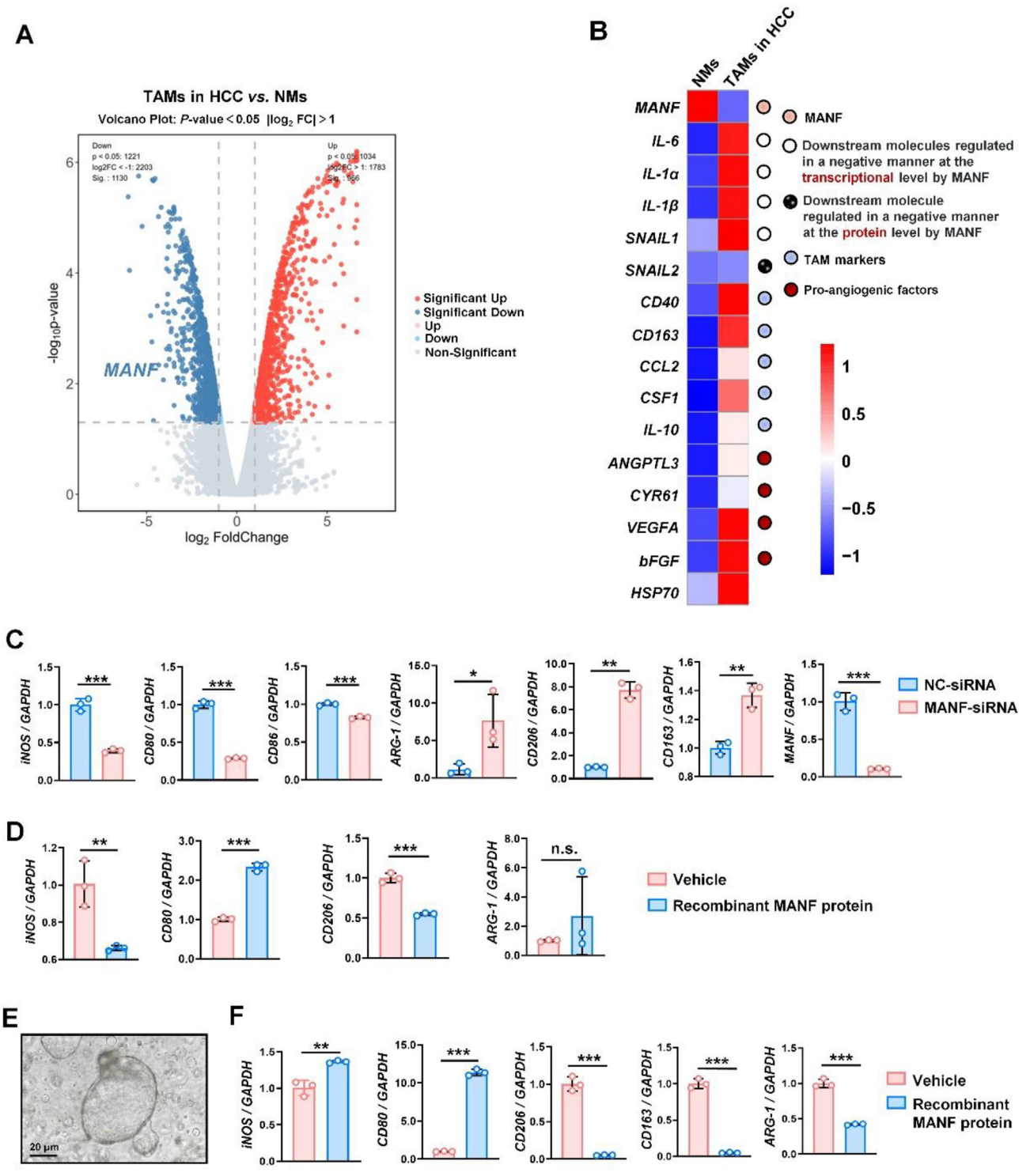


**Figure 1** MANF reprograms TAMs into M1 phenotype. Volcano plot (A) and heatmap (B) of RNA sequencing data (GSE158792) between TAMs in HCC and NMs. TAMs: tumor associated macrophages. NMs: normal macrophages. (C) PMA-treated THP-1 cells were transfected with MANF-siRNA or NC-siRNA. qPCR analysis was performed 48 h after transfection to detect the markers of M1 phenotype and M2 phenotype. (D) PMA-treated THP-1 cells were treated with recombinant MANF protein at dosage of 8 μg/mL. qPCR analysis was performed 48 h after MANF treatment to detect the markers of M1 phenotype and M2 phenotype. (E) HCC organoids were cultured and the cultural supernatant was collected. (F) PMA-treated THP-1 cells were treated with recombinant MANF protein (8 μg/mL) and HCC organoid cultural supernatant. Forty-eight hours later, cells were harvested for qPCR analysis to detect the markers of M1-phenotype or M2-phenotype TAMs. Data are present as mean ± SD, $*P < 0.05$, $**P < 0.01$, $***P < 0.001$, $n = 3$.

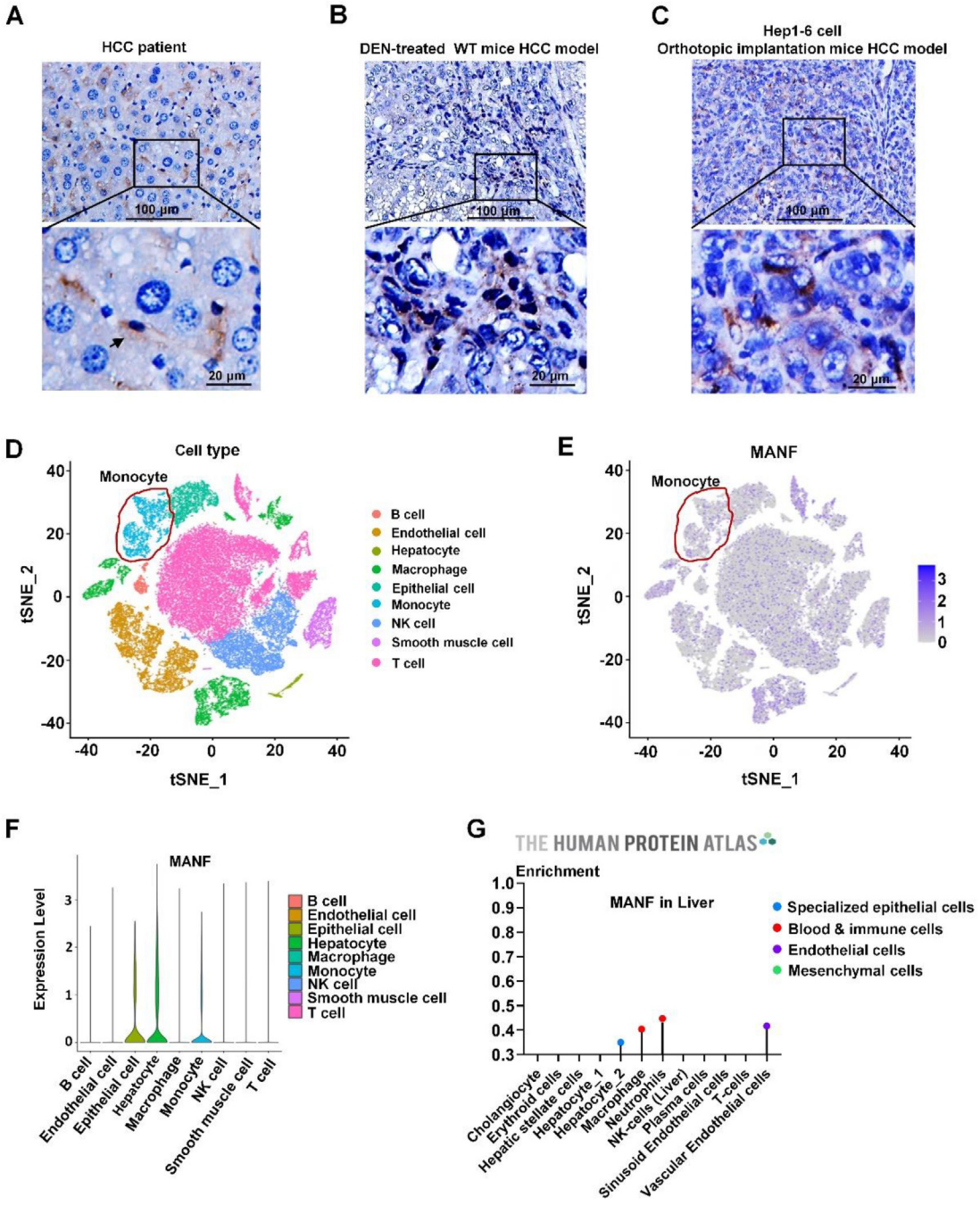


**Figure 2** High level of MANF in monocytes/macrophages of liver tissues. (A–C) High levels of MANF in nonparenchymal cells in liver. Immunohistochemical staining of MANF expression in the liver cancer tissues of HCC patient (A), DEN-treated mice HCC model (B), and Hep1-6 cells-related orthotopic implantation mice HCC model (C). (D–G) Analysis of MANF expression in human liver tissues. (D–F) Analysis of single cell sequencing data from GSE156625. (D) Dimensionality reduction using tSNE shows cellular heterogeneity of liver tissues from HCC patient. (E) t-SNE nonlinear dimensionality reduction to display the differential expression of *MANF* gene in various cell types of liver tissues. (F) Violin plot of *MANF* gene expression in various cell types of liver tissues. (G) Analysis of MANF level in various cells of liver tissues from The Human Protein Atlas database.

deficiency decreased the levels of M1-phenotype markers (*iNOS*, *CD80* and *CD86*) and increased the levels of M2-phenotype markers (such as *ARG-1*, *CD206*, *CD163*, Fig. 1C). We also used recombinant MANF protein to treat PMA-treated THP-1 cells, and found that MANF supplement decreased the levels of *iNOS* and *CD206* and increased *CD80* level, but had no effect on *ARG-1* level (Fig. 1D), suggesting that recombinant MANF did not effectively increase all M1 markers and suppress all M2 markers because of lack of tumor microenvironment-induced M2-like phenotype of TAMs. To investigate the effect of MANF on TAMs, we cultured HCC organoid and used the organoid culture medium to treat macrophages in order to transform NMs to TAMs.

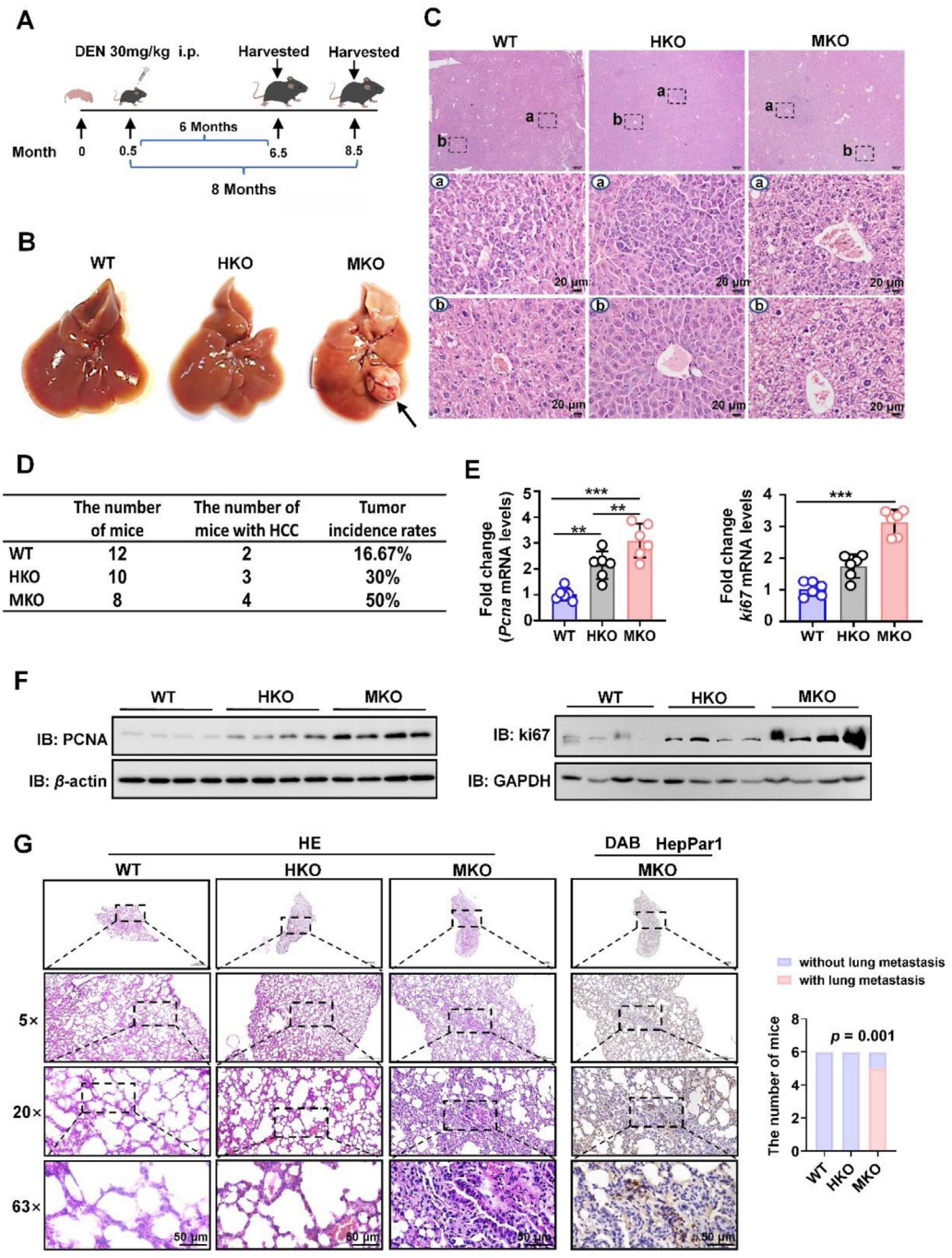


**Figure 3** Myeloid-specific deletion of *Manf* gene promotes HCC. Myeloid-specific deletion of *Manf* gene male mice (MKO), hepatocyte-specific *Manf* gene deletion male mice (HKO) and their control mice (wild type mice, WT) were injected intraperitoneally (i.p.) with DEN (30 mg/kg) at day 15 postpartum. Mice were harvested 6 or 8 months after DEN treatment. (A) Scheme of DEN-induced HCC mice model. (B) Photograph of typical livers from WT, HKO, MKO mice at 6 months of DEN treatment. The black arrow indicated the tumor on the surface of mice liver. (C) HE staining of liver sections from WT, HKO and MKO mice at 6 months after DEN treatment. The images of the rectangles in upper panels are magnified in the middle and bottom panels. Middle panels: cancer foci; bottom panels: para-cancer tissues. (D) The tumor incidence rates of mice at 6 months after DEN treatment. The incidence of tumor was diagnosed by HE staining of liver tissues, and then the incidence rates were calculated. (E, F) PCNA and ki67 levels in the liver tissues of *Manf* gene deletion mice. qPCR (E) and Western blot (F) were used to detect the mRNA and protein levels in the liver tissues of DEN-treated mice. (E) Data are presented as mean ± SD, $n = 6$, $^{**}P < 0.01$, $^{***}P < 0.001$. (G) HE staining of lung sections from WT, HKO and MKO mice at 8 months after DEN treatment. DAB staining of HepPar1 was detected in the lung section of MKO mice to verify lung metastasis of hepatoma cells. Statistical result of HCC lung metastasis was shown in right panel. $n = 6$, $P = 0.001$, MKO *vs*. WT.

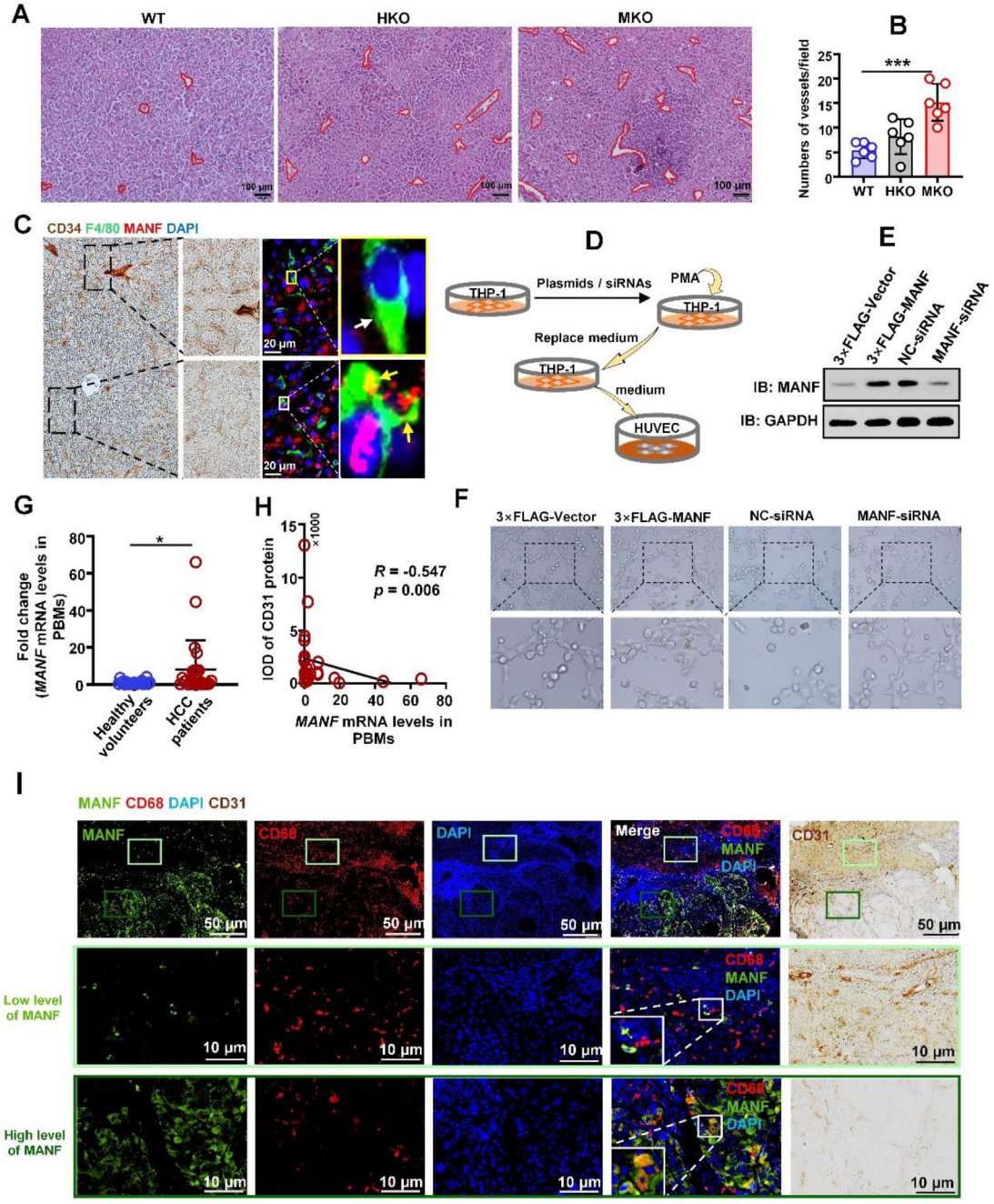


**Figure 4** Deficiency of MANF promotes neovascularization. (A−C) Myeloid-specific deletion of *Manf* gene promoted neovascularization. WT, HKO and MKO mice were harvested at 6 months, after DEN treatment. (A, B) HE staining of liver tissues. The number of blood vessels was calculated at the same magnified field (10 × objective plus 10 × eyepiece). Panel B is the statistical data of panel A. Data are presented as mean ± SD. ***$P < 0.001$, $n = 6$. (C) Liver section from DEN-treated WT mice was co-stained with CD34 (brown), F4/80 (green) and MANF (red). DAPI was used to detect nuclei. Upper panels: liver tissue with a high level of CD34 expression and a low level of F4/80$^+$ cells-derived MANF. Bottom panels: liver tissue with a low level of CD34 expression and a high level of F4/80$^+$ cells-derived MANF. White arrow indicated as macrophage without MANF expression; yellow arrows indicated as macrophages with MANF protein. Scale bars: 20 μm. (D−F) Macrophages-derived MANF suppressed tube formation of HUVEC cells. THP-1 cells were transfected with 3 × FLAG-MANF, MANF-siRNA and corresponding controls, respectively. Twenty-four hours later, cells were treated with 100 ng/mL PMA for 24 h, and then the culture medium was changed. The medium of THP-1 was collected 24 h later to culture HUVEC cells. (D) Scheme of this experiment. (E) The efficiency of transfection in THP-1 cells. (F) The morphology of HUVEC cells was observed 2 h later. (G−I) Clinical data about the effect of MANF on HCC. (G) PBMs were extracted from 24 HCC patients and 21 healthy volunteers for qPCR assay to detect *MANF* mRNA levels. *$P < 0.05$. (H) PBMs were extracted for qPCR assay to detect *MANF* mRNA level. Immunohistochemistry staining of CD31 was performed in the liver cancer tissues from the same HCC patient, and IOD of CD31 was calculated. The relationship was analyzed between *MANF* mRNA level in PBMs and CD31 protein level in liver tissues. $R = -0.547$, $P = 0.006$. $n = 24$. (I) Liver cancer section of HCC patient was co-stained with MANF (green), CD68

Under these conditions, recombinant MANF supplement increased the levels of M1-phenotype markers (*iNOS*, *CD80*) and reduced the levels of M2-phenotype markers (*CD206*, *CD163*, *ARG-1*) (Fig. 1E and F). These data suggested that MANF attenuated M2-like phenotype and increased M1-like phenotype of TAMs, suggesting that MANF reprogramed TAMs *in vitro*.

### 3.2. Loss of MANF in hepatic macrophages promotes HCC

Since above-mentioned data indicated that MANF reprogramed TAMs into M1-like phenotype, we speculated MANF in hepatic macrophages might suppress HCC progression. Our previous study described that hepatocyte-derived MANF inhibited epithelial-mesenchymal transition (EMT) of HCC[14]. Therefore, we investigated MANF expression in all cells of HCC tissues. We found high protein levels of MANF in nonparenchymal cells of liver tissues from HCC patient, DEN-induced mouse HCC model and Hep1-6 cells-related orthotopic implantation mouse HCC model (Fig. 2A–C). Next, single-cell sequencing[17] was downloading from GEO database (GSE156625) to detect *MANF* expression in various cells of liver tissues from HCC patient. The data showed that *MANF* mRNA level was highly expressed in monocytes, close to hepatocytes (Fig. 2D–F). We also investigated MANF expression in all cells of liver with The Human Protein Atlas database, and found the high level of MANF in hepatic macrophages (Fig. 2G).

On the one hand, liver injury of HCC tissues led to the recruitment of PBMs to supply hepatic macrophage[18], and *MANF* mRNA level was highly expressed in monocytes, close to hepatocytes (Fig. 2D–F). One the other hand, data from The Human Protein Atlas database exhibited high level of MANF in hepatic macrophages (Fig. 2G). Therefore, the proportion of MANF in monocyte-derived macrophages (MDMs) was high in liver tissues. Next, we constructed myeloid cell-specific MANF knockout (MKO) mice to investigate the effect of MDMs-derived MANF on HCC progression and used hepatocyte-specific knockout (HKO) mice as a control in current study. HKO, MKO and their control (WT) mice were utilized to establish DEN-induced HCC mouse model (Fig. 3A). Evaluation of tumor incidence by HE staining indicated that tumor incidence rate of HCC in MKO mice was higher than that of WT and HKO mice (Fig. 3C and D). Meanwhile, the tumor on the liver surface of MKO mice was appeared, but not WT and HKO mice at 6 months after DEN treatment (Fig. 3B), and the levels of PCNA and ki67, biomarkers for proliferation, were higher than those of WT and HKO mice (Fig. 3E and F, Supporting Information Fig. S2A–S2D). The effect of MANF on the apoptosis was then evaluated by TUNEL staining, and the apoptosis rate of hepatocytes was much lower in MKO mice than that in WT mice (Fig. S2G and S2H). Morphological data revealed that the proliferation ability of primary hepatocytes extracted from DEN-treated MKO mice was greater, compared with that of WT mice (Fig. S2E). Furthermore, the higher viability of primary hepatocytes in DEN-treated MKO mice than in WT mice (Fig. S2F) was verified. Additionally, the incidence of lung metastasis in MKO mice was increased, compared with WT and HKO mice at 8 months after DEN treatment (Fig. 3G). These data indicated that *Manf* gene knockout in myeloid cells increased the proliferation of primary hepatocytes, and inhibited its apoptosis, promoting lung metastasis, leading to tumor progression.

### 3.3. Loss of MANF in hepatic macrophages promotes HCC neovascularization

As the above-mentioned data demonstrated that MANF derived from myeloid cells was involved in the regulation of the proliferation, viability, and apoptosis of hepatocytes in DEN-induced mice HCC model, it was important to define the mechanism underlying its effects that influenced many characteristics of hepatocytes. MANF reprograming TAMs was verified *in vitro*, and next *in vivo* analysis needs to be investigated. The data from DEN-induced mice HCC model indicated that MANF deficiency exhibited reduction of M1-phenotype and up-regulation of M2-phenotype (Supporting Information Fig. S3A and S3B), suggesting that MANF reprogramed TAMs into M1 phenotype *in vivo*.

Meanwhile, given that MKO mice had more pronounced neovascularization in the cancer nest compared to WT and HKO mice (Fig. 3C), the effect of myeloid cells-derived MANF on tumor neovascularization in HCC was next investigated with the hypothesis that *Manf* gene knockout in myeloid cells could promote neovascularization. The number of blood vessels in the same magnified field (10 × objective plus a 10 × eyepiece) was calculated in the liver tissues of DEN-treated WT, HKO, and MKO mice. The data indicated that the number of blood vessels in MKO mice was higher than in WT and HKO mice (Fig. 4A and B). Consistently, the level of CD31, a marker of vascular epithelial cells, was up-regulated in liver tissues of MKO mice compared to that of WT and HKO mice (Supporting Information Fig. S4A–S4D). We also investigated the relationship of hepatic macrophage-derived MANF and tumor neovascularization in one section of liver tissue in order to avoid the influence of immunohistochemical staining conditions on experiment results. Liver section of DEN-treated WT mice was used to perform immunohistochemistry staining of CD34 (marked blood vessels) followed by co-staining with F4/80$^+$ (marked hepatic macrophages) and MANF. The data revealed that higher CD34 level in the liver tissues coincided with lower MANF levels in F4/80$^+$ macrophage (upper panels of Fig. 4C, white arrow indicated as macrophage with no MANF expression), while lower CD34 level accompanied by higher MANF levels in F4/80$^+$ macrophages (bottom panels of Fig. 4C, yellow arrows indicated as macrophages with high level of MANF). These data suggest that loss of MANF in hepatic macrophage might play a promotive role in the regulation of HCC neovascularization.

### 3.4. The level of MDMs-derived MANF is negatively correlated with neovascularization of HCC

Hepatic macrophages consist of resident macrophages termed Kupffer cells (KCs) and MDMs[18]. Although resident KCs are the predominant macrophages in the normal liver, the number of KCs decreases in liver diseases, accompanied by an increase in the number of MDMs recruited from peripheral blood[18]. Thus, the

(red), DAPI (blue) and CD31 (brown). Middle panels (with light green rectangles) were the enlarged images of the light green rectangles from upper panels, which were the liver tissue with a low level of CD68$^+$ macrophages-derived MANF and a high level of CD31 expression. Bottom panels (with dark green rectangles) were the enlarged images of the dark green rectangles from upper panels, which were the liver tissue with a high level of CD68$^+$ macrophages-derived MANF and a low level of CD31 expression. Scale bars were shown as indicated in the images.

effect of MDMs-derived MANF on neovascularization and TAMs reprograming was next investigated.

First, we used THP-1 cells, a cell line of monocyte, to modulate the expression of *MANF* gene using *RNAi* or overexpression systems. After treatment of THP-1 cells with PMA to induce differentiation into macrophages, cell culture medium of MDMs was collected and used for culturing HUVEC cells in order to investigate the effect of MANF in macrophages on

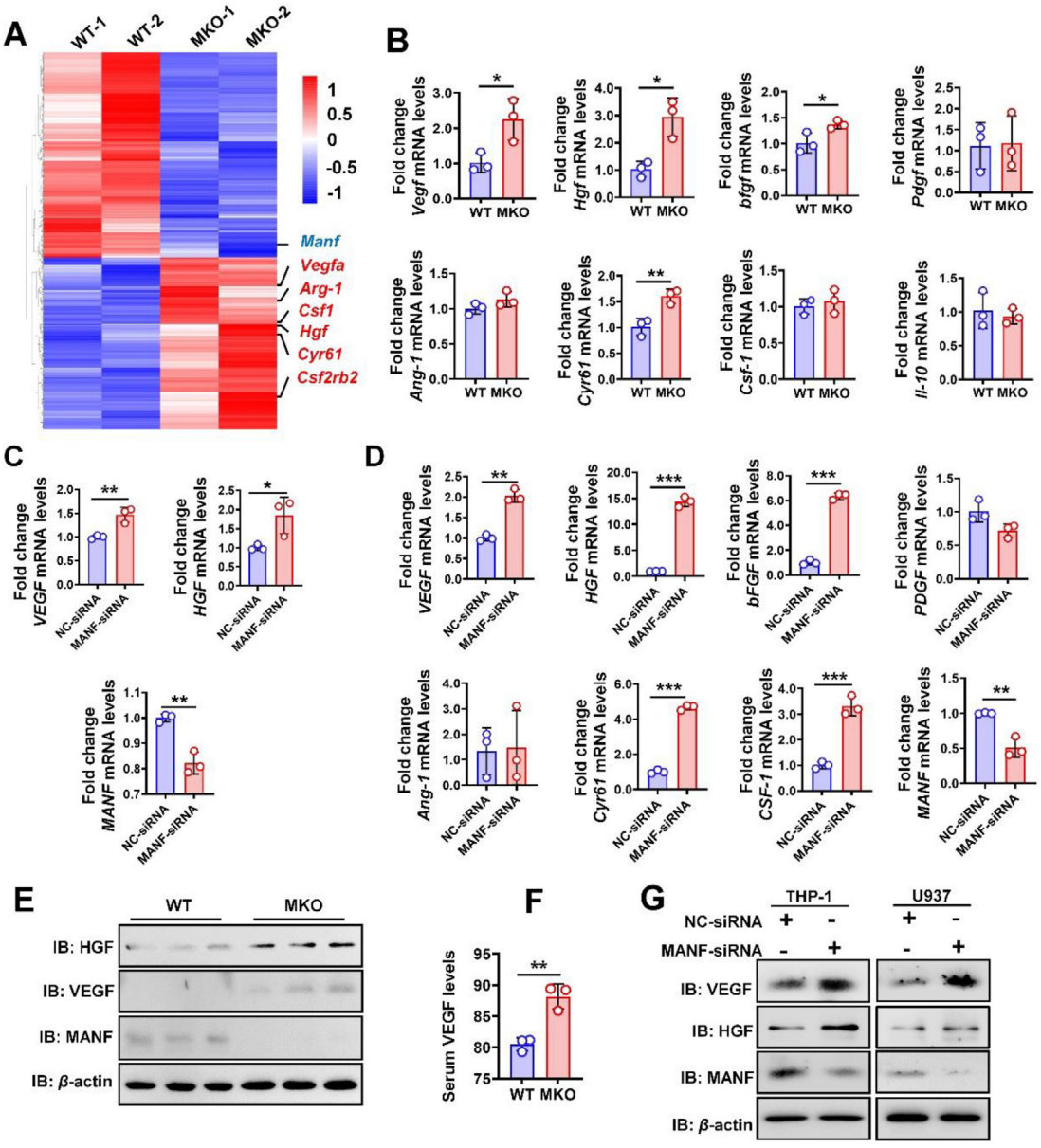


**Figure 5** Deficiency of MANF increases pro-angiogenic factors levels in macrophages. (A) RNA sequencing analysis of angiogenic factors levels in peritoneal macrophages extracted from MKO mice and its control WT mice. (B) Primary hepatic macrophages were extracted from WT and MKO mice at 6 months after DEN treatment. qPCR assay was performed to detect the mRNA levels of various pro-angiogenic factors. Data are presented as mean ± SD. $^{*}P < 0.05$, $^{**}P < 0.01$, $n = 3$. (C) U937 cells were transfected with MANF-siRNA or NC-siRNA for 48 h and treated with 100 ng/mL PMA for 24 h. After that, cells were cultured in a hypoxic environment (1% $O_2$) for 2 h for qPCR assay to detect the mRNA levels of *VEGF* and *HGF*. *MANF* mRNA level was also detected to estimate the transfection efficiency. $^{*}P < 0.05$, $^{**}P < 0.01$, $n = 3$. (D) THP-1 cells were transfected with MANF-siRNA or NC-siRNA for 48 h and treated with 100 ng/mL PMA for 24 h. After that, cells were cultured in a hypoxic environment (1% $O_2$) for 24 h for qPCR assay to detect the mRNA levels of various pro-angiogenic factors. *MANF* mRNA level was also detected to estimate the transfection efficiency. $^{**}P < 0.01$, $^{***}P < 0.001$, $n = 3$. (E) Primary hepatic macrophages were extracted from WT and MKO mice at 6 months after DEN treatment. Western blot assay was performed to detect the protein levels of HGF and VEGF. (F) Serum was collected from WT and MKO mice at 6 months after DEN treatment for ELISA assay to detect serum VEGF level. $^{**}P < 0.01$, $n = 3$. (G) THP-1 cells and U937 cells were transfected with MANF-siRNA or NC-siRNA for 48 h and treated with 100 ng/mL PMA for 24 h. After that, cells were cultured in a hypoxic environment (1% $O_2$) for 24 h for Western blot assay to detect VEGF and HGF protein levels.

neovascularization *in vitro*. The data revealed that loss of MANF in MDMs accelerated neovascularization *in vitro* (Fig. 4D–F).

Then, the effect of MANF on TAMs was estimated in clinical specimens. We extracted PBMs from 21 health volunteers and 24 HCC patients. The *MANF* mRNA level of PBMs was found to be higher in HCC patients than in healthy volunteers (Fig. 4G). We also found that low level of MANF in PBMs exhibited the decrease of M1-phenotype and the increase of M2-phenotype in TAMs (Supporting Information Fig. S5). Then, we investigated the effect of *MANF* level in PBMs on the neovascularization of HCC patients. While CD31 protein levels was higher in liver tissues of HCC patients with low level of *MANF* in PBMs, HCC patients with high level of *MANF* in PBMs had lower CD31 protein levels in the liver tissues (Fig. S4E). Further data revealed a negative correlation between *MANF* mRNA level in PBMs and CD31-positive immunostaining in the liver tissues of HCC patients (Fig. 4H, $R = -0.547$, $P = 0.006$), suggesting that *MANF* mRNA level in PBMs might inhibit liver cancer neovascularization of patients. Additionally, we used CD68 to mark human liver macrophages, and investigated MANF levels in $CD68^+$ macrophages. The data indicated that high CD31 levels coincided with low MANF levels in $CD68^+$ macrophages (light green rectangles in Fig. 4I), while low CD31 levels were accompanied by high MANF levels in $CD68^+$ macrophages (dark green rectangles in Fig. 4I). These clinical data suggested that MDMs-derived MANF might inhibit HCC neovascularization.

### 3.5. *MDMs-derived MANF reduces pro-angiogenic factors levels*

To investigate the mechanism underlying the effect of MDMs-derived MANF in HCC neovascularization, peritoneal macrophages were extracted from MKO mice and its control WT mice, and RNA sequencing were performed. As sequencing data revealed that *Manf* gene knockout increased various pro-angiogenic factors (*Vegf, Hgf, Csf1, Cyr61, Csf2rb2*) and TAMs marker (*Arg-1*) (Fig. 5A), we also investigated the effect of MANF on the levels of vascular growth factors *in vivo* and *in vitro*. Hepatic macrophages were extracted from DEN-treated MKO and WT mice for analysis of angiogenic factors levels. Consistent with RNA-seq data, myeloid cell-specific knockout of *MANF* gene increased the mRNA levels of several pro-angiogenic factors, including *Vegf*, *Hgf, bfgf*, and *Cyc61* (Fig. 5B). Furthermore, we also explored the effect of MDMs-derived MANF on the levels of these angiogenic factors in cell lines. Some angiogenic factors, including *HGF*, *PDGF,* and *CSF-1* mRNA levels but not *VEGF* were increased when U937 cells transfected with MANF-siRNA (Supporting Information Fig. S6). As hypoxia is a common feature in the microenvironment of HCC, the effect of MANF on angiogenic factors levels in hypoxia-treated macrophages was evaluated. The data revealed that the knockdown of *MANF* increased the mRNA levels of several angiogenic factors, including *VEGF* and *HGF*, under hypoxic condition (Fig. 5C and D).

To investigate the effect of MANF on the protein levels of VEGF and HGF in macrophages, hepatic macrophages were extracted from DEN-treated WT and MKO mice, and HGF and VEGF protein levels were evaluated. The myeloid-cell specific knockout of MANF increased cellular HGF and VEGF levels (Fig. 5E), as well as serum VEGF levels (Fig. 5F). *In vitro* data also verified that knockdown of MANF in THP-1 or U937 cells increased VEGF and HGF levels (Fig. 5G). Altogether, our data suggested that MDMs-derived MANF inhibited pro-angiogenic factors levels.

### 3.6. *MANF interacts with HSP70-1 and negatively regulates its expression in macrophages*

In our previous study, immunoprecipitation-coupled mass spectroscopy (IP-MS) was utilized to identify the potential interacting protein partners of MANF[19]. The IP-MS based proteomics data indicated that MANF may interact with heat shock protein 70-1 (HSP70-1), which is associated with macrophage-mediated neovascularization as the levels of VEGF and HGF were increased in macrophages treated with recombinant HSP70-1 protein[20]. Similarly, the levels of various pro-angiogenic factors (such as *VEGF, HGF* and *bFGF* ) and TAMs markers (such as *CD206, CD163* and *ARG-1*) were increased in THP-1 cells that overexpressed HSP70-1 (Supporting Information Fig. S7). The proteomics result indicating potential protein–protein interaction of MANF with HSP70-1 was validated first by performing GST-pull down assay (Fig. 6A and B). Furthermore, MANF and HSP70 were co-localized in PMA-treated THP-1 and U937 cells (Fig. 6C and E), and their presence in the same intracellular complex was verified by Co-IP experiments using macrophage cell lines (Fig. 6D and F) and primary hepatic macrophages (Fig. 6G). These data showed that MANF directly interacted with HSP70-1.

Besides their direct interaction, as our immunofluorescence data revealed that the level of HSP70 was decreased in macrophage with a high level of MANF (Fig. 6C and E, indicated by white arrows), the possible correlation between expression of MANF and HSP70-1 was evaluated in macrophages. The myeloid-cell specific knockout of MANF in MKO mice resulted in elevated mRNA and protein levels of HSP70-1 in the primary hepatic macrophages compared to WT mice (Fig. 6H and I). Immunohistochemical analysis of HSP70 in the liver tissues of WT, HKO, and MKO mice treated with DEN revealed increased HSP70-1 protein level of liver tissues in MKO mice, especially in the non-parenchymal cells (Supporting Information Fig. S8A and S8B). Due to the increase of HSP70-1 levels in hepatic macrophages of MKO mice (Fig. 6H and I), we speculated that non-parenchymal cells with increased levels of HSP70-1 protein in Fig. S8A may be liver macrophages. To determine the type of non-parenchymal cells with increased HSP70-1 levels, F4/80 was used to mark macrophages in the liver tissues of DEN-treated MKO mice. Our data revealed that HSP70 was indeed localized in $F4/80^+$ cells (Fig. S8C), suggesting once again that MANF decreased HSP70 levels in hepatic macrophages of mouse HCC model. Silencing MANF expression in U937 and THP-1 cells also increased not only mRNA levels but also intracellular protein levels of HSP70 (Fig. 6J–M, Supporting Information Fig. S9A). Conversely, treatment of cells with recombinant MANF protein as well as overexpression of MANF diminished mRNA and protein expression of HSP70-1 (Fig. 6N–O, Fig. S9B and S9C). These findings indicated that MANF negatively regulated HSP70-1 expression in macrophages.

### 3.7. *MANF inhibits the nuclear import of HSF1 in macrophages*

Expression of HSP70-1 is mainly regulated by heat shock factor I (HSF1), a transcription factor that binds to heat shock transcription control element[21]. Stress-induced dissociation of HSP70-1 from HSF1 allows HSF1 to translocate to nuclei where it acts as a transcription factor, resulting in increased mRNA levels of *HSP70-1*, which in turn represses HSF1 activity[21] (Fig. 7A). As

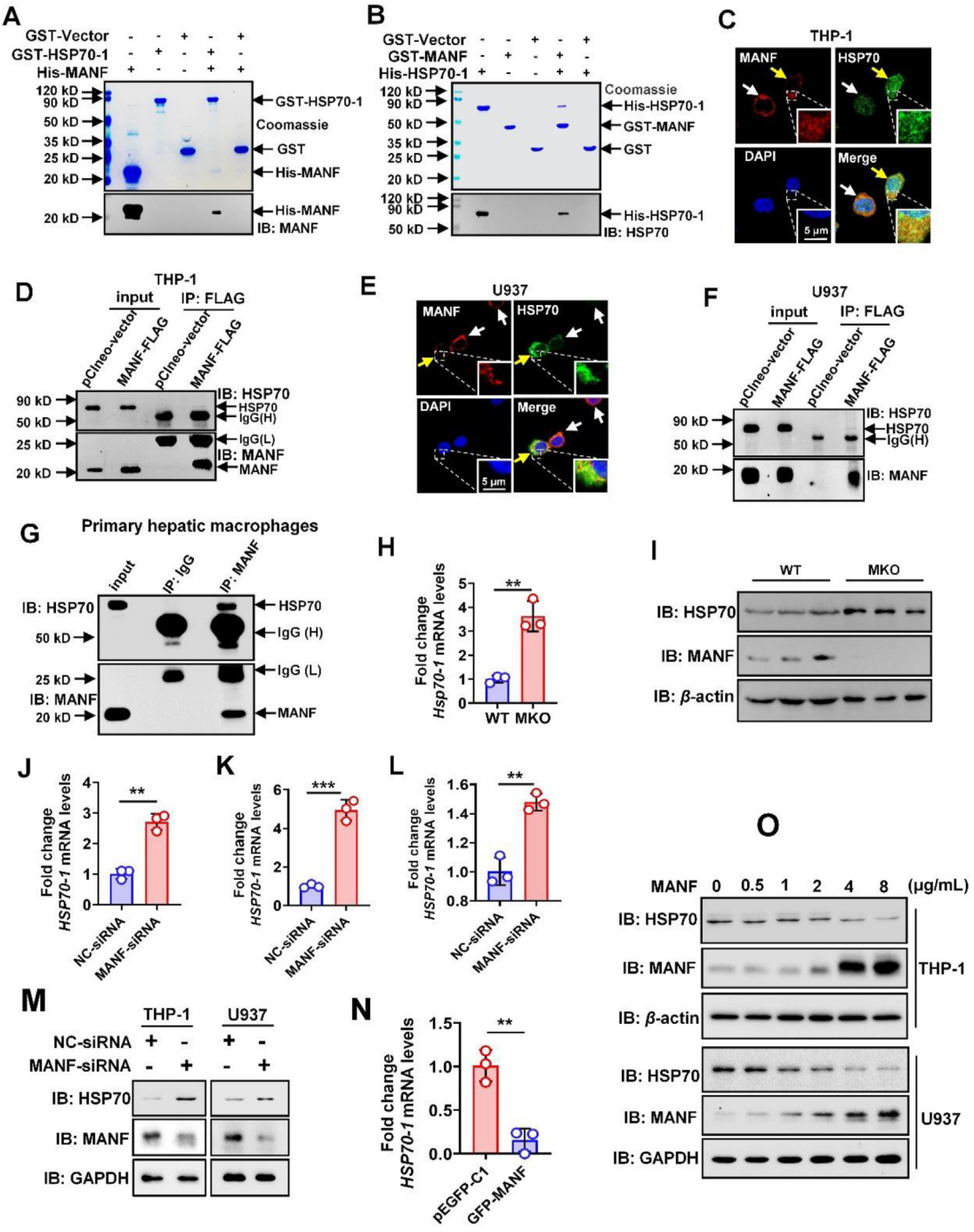


**Figure 6** MANF decreases HSP70-1 level. (A, B) GST-pull down experiment was used to identify the direct interaction of MANF and HSP70-1. (C) Co-localization of MANF and HSP70-1. THP-1 cells were treated with 100 ng/mL PMA for 24 h, and then immunofluorescence assay was performed with MANF (red) and HSP70 (green) antibodies. The nuclei were detected with DAPI (blue). White arrows: high level of MANF and low level of HSP70; yellow arrows: low level of MANF and high level of HSP70. Scale bar: 5 μm. (D) Co-IP assay was used to verify the interaction of MANF and HSP70-1 in PMA-treated THP-1 cells. (E) Co-localization of MANF (red) and HSP70 (green) in PMA-treated U937 cells. White arrows: high level of MANF and low level of HSP70; yellow arrows: low level of MANF and high level of HSP70. Scale bar: 5 μm. (F) Co-IP assay was used to verify the interaction of MANF and HSP70 in PMA-treated U937 cells. (G) Primary hepatic macrophages were extracted from DEN-treated WT mice for analyzing the interaction of MANF and HSP70. Co-IP assay was performed with anti-MANF antibody, and rabbit IgG antibody was used as a negative control. (H, I) Primary hepatic macrophages were extracted from DEN-treated WT mice and MKO mice for qPCR (H) and Western blot (I) assays to detect HSP70-1 levels. $^{**}P < 0.01$, $n = 3$. (J–L) U937 (J) and THP-1 cells (K, L) were transfected with NC-siRNA or MANF-siRNA, treated with PMA for 24 h and hypoxia for 2 h (J), 24 h (K) or 48 h (L). Then, qPCR assay was performed. $^{**}P < 0.01$, $^{***}P < 0.001$, $n = 3$. (M) THP-1 and U937 cells were transfected with NC-siRNA or MANF-siRNA, treated with PMA and hypoxia for 24 h. Cells were collected for Westen blot assay to detect HSP70 levels. (N) THP-1 cells were transfected with pEGFP-C1 or GFP-MANF and treated with PMA for 24 h. HSP70-1 mRNA level was detected with qPCR assay. $^{**}P < 0.01$, $n = 3$. (O) THP-1 and U937 cells were treated with recombination MANF protein at different dose as indicated for 48 h. Cells were collected for Western blot assay to detect HSP70 levels.

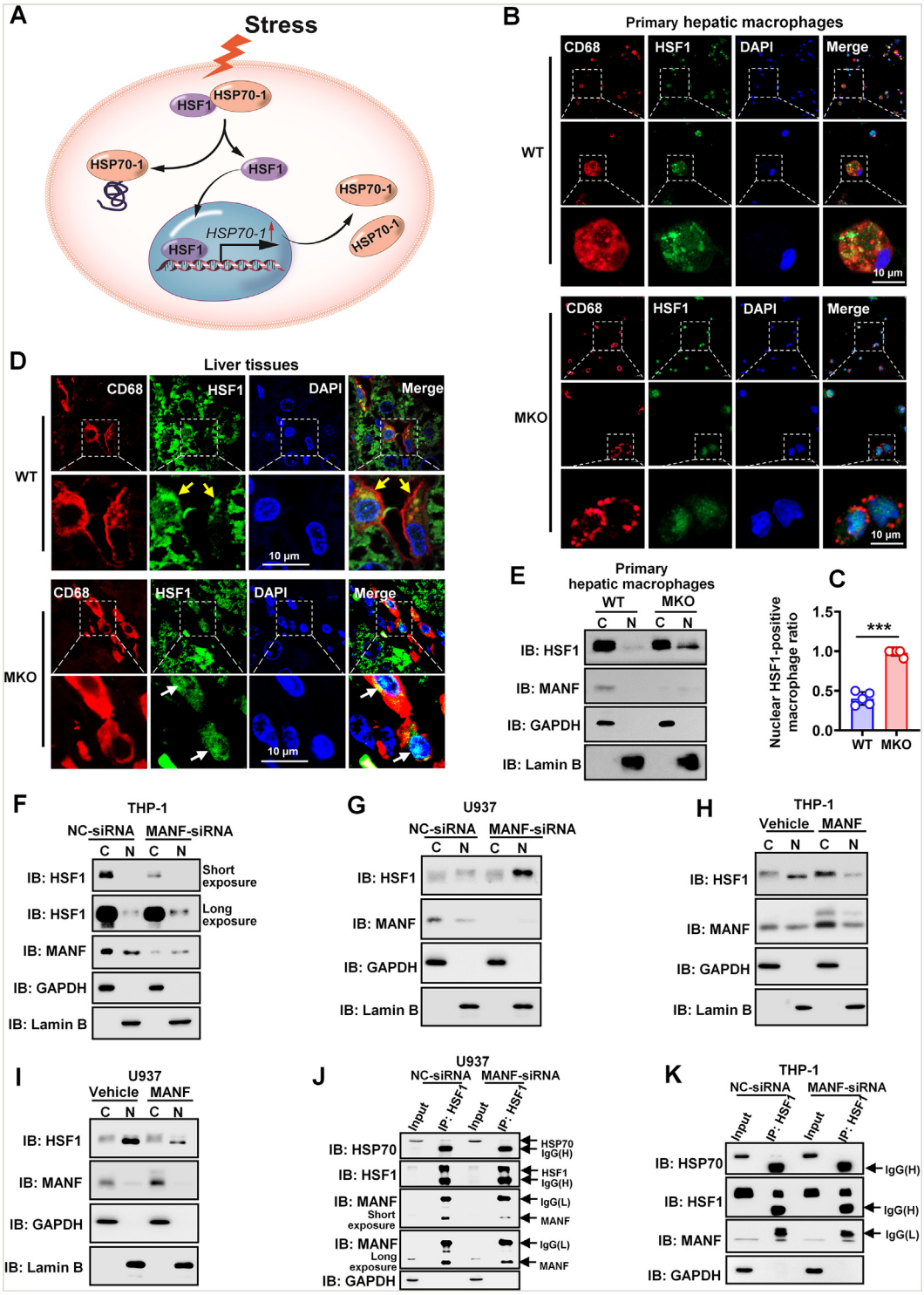


**Figure 7** MANF inhibits the nuclear import of HSF1 in macrophages. (A) Schematic diagram of HSF1 regulating the transcription of HSP70-1. (B−D) MANF deficiency promotes HSF1 nuclear import in CD68$^{+}$ macrophages. Immunofluorescence was performed to detect CD68 (red) and HSF1 (green) in primary hepatic macrophage (B) and liver sections (D) of DEN-treated WT and MKO mice. Panel C is the statistical data of panel B. Yellow arrows indicated that HSF1 was almost localized in the cytoplasm of WT mice; white arrows indicated the nuclear import of HSF1 of MKO mice. Scale bars: 10 μm. (E−G) MANF deficiency increased HSF1 nuclear import in primary hepatic macrophages (E), PMA-treated THP-1 (F) and U937 cells (G) as indicated. Cytoplasmic protein and nuclear protein were extracted to perform Western blot. C, cytoplasmic protein; N, nuclear protein. (H, I) Recombinant MANF protein reduced HSF1 nuclear translocation. THP-1 (H) and U937 (I) cells were treated with or without 8 μg/mL recombinant MANF protein. After PMA treatment, cytoplasmic protein and nuclear protein were extracted to perform Western blot. (J, K) U937 (J) and THP-1 (K) cells were transfected with NC-siRNA or MANF-siRNA, and treated with PMA. Co-IP was performed with anti-HSF1 antibody. Western blot was performed to investigate the effect of MANF knockdown on the interaction of HSF1−HSP70.

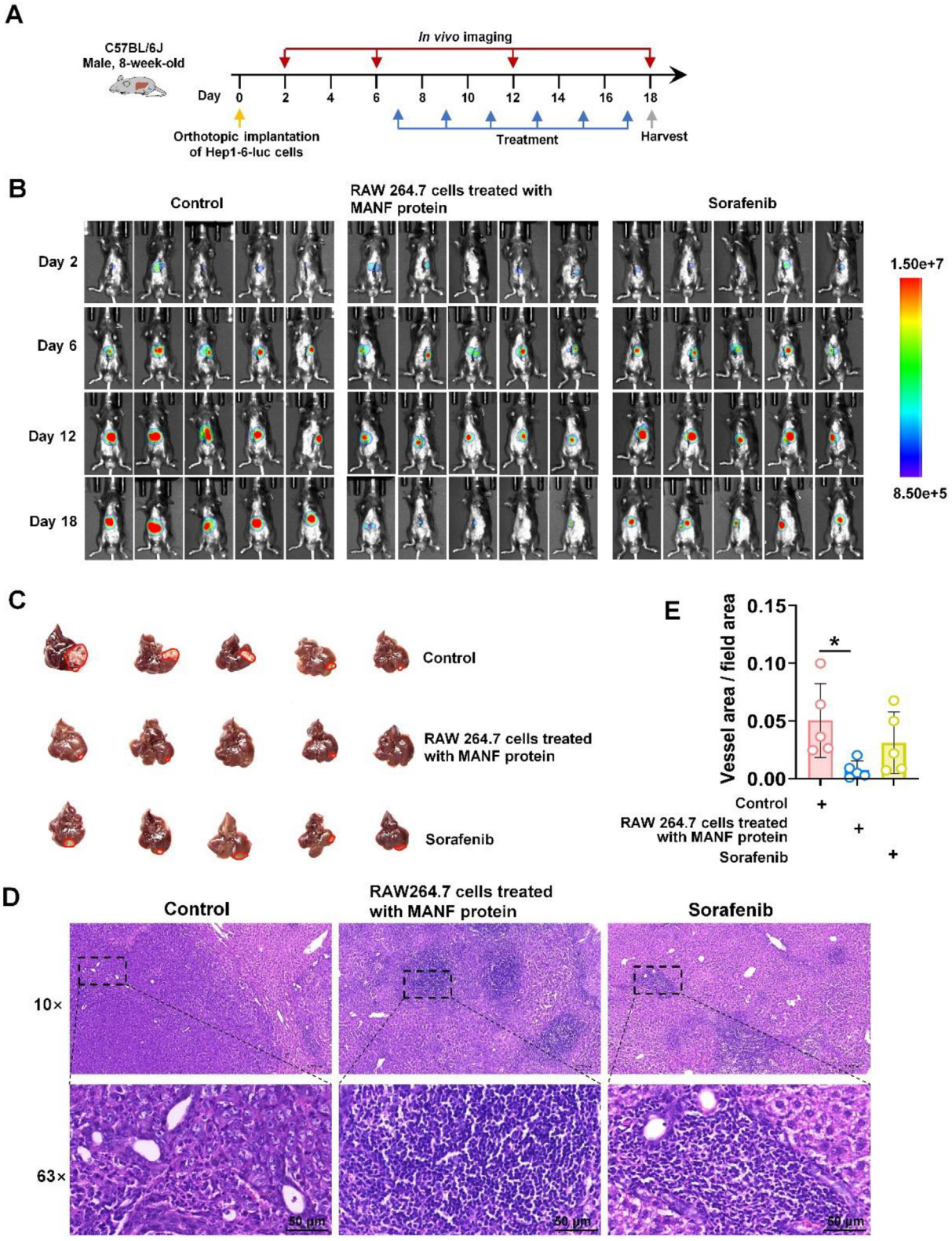


**Figure 8** MDMs-derived MANF suppresses HCC progression. Eight-week-old C57BL/6J male mice were orthotopic injected with Hep1-6-Luc cells. RAW 264.7 cells were treated with recombinant His-MANF protein (32 μg/mL) for 24 h and then injected to mice through tail vein. Sorafenib (5 mg/kg) was used as a positive control by intravenous injection. Control group is the negative control. (A) Scheme of orthotopic implantation mice HCC model. (B) *In vivo* imaging of mice. (C) Photograph of mice livers from orthotopic implantation model after harvest. (D) HE staining of liver tissues. (E) The statistical data of tumor neovascularization between 3 groups. $^*P < 0.05$, $n = 5$.

MANF interacts with HSP70-1 and regulates its expression levels in macrophages, the potential effect of MANF on feedback loop of HSP70-1 and HSF1 was investigated. First, the subcellular localization of HSF1 was evaluated in the primary hepatic macrophages extracted from DEN-treated WT and MKO mice. HSF1 was localized in the cytoplasm of $CD68^+$ hepatic macrophages of DEN-treated WT mice, whereas it was localized in the nuclei of $CD68^+$ hepatic macrophages of DEN-treated MKO mice (Fig. 7B and C), suggesting that the knockout of MANF promoted the nuclear import of HSF1 protein. Similarly, immunohistochemistry staining of liver sections revealed that $CD68^+$ hepatic macrophages of DEN-treated MKO mice had higher nuclear HSF1 protein levels compared to that of WT mice (Fig. 7D). The immunoblot results of fractionation assay further indicated that MANF deficiency increased HSF1 nuclear import (Fig. 7E). The effect of MANF on the subcellular localization of HSF1 was also assessed *in vitro*. Silencing of MANF expression in THP-1 and U937 cells promoted HSF1 nuclear import (Fig. 7F and G, Supporting Information Fig. S10A), whereas treatment with recombinant MANF protein or overexpression of MANF inhibited HSF1 nuclear translocation (Fig. 7H and I, Fig. S10B).

Considering the effect of MANF on the regulation of HSP70-1 level and HSF1 nuclear translocation as well as the requirement for dissociation of HSF1/HSP70-1 complex to facilitate nuclear import of HSF1, the possible role of MANF in the HSP70-HSF1 feedback loop was next investigated. Silencing of MANF expression both in U937 and THP-1 cells reduced the interaction between HSF1 and HSP70 (Fig. 7J and K), suggesting that MANF enhances HSF1-HSP70 interaction, which in turn restricts nuclear translocation of HSF1 and reduces HSP70-1 levels.

### *3.8. Recombination MANF supplement in MDMs is an effective treatment for HCC*

Since above-mentioned data indicated that loss of MANF in MDMs promotes HCC progression, we next investigated whether MANF supplement in MDMs suppressed HCC or not. Different dosages of recombination MANF protein were added to the culture medium of mice monocyte cell line (RAW 264.7), and RAW 264.7 cells were detected MANF levels in order to choose an appropriate dosage (Supporting Information Fig. S11A). Then, RAW 264.7 cells treated with exogenous His-MANF protein, were intravenous injected to treat mice liver orthotopic implantation HCC model with Hep1-6-luc cells. Sorafenib was used as a positive drug for HCC treatment (Fig. 8A–E). His-MANF protein was detected in hepatic macrophages (Supporting Information Figs. S11B, S12A, S12B, S13A, S13B), that indicated the recruitment of RAW 264.7 cells to liver tissues and differentiate into hepatic macrophages. For mice with orthotopic implantation tumor cells, the exogenous His-MANF protein in RAW 264.7 cells were MDMs-derived MANF supplement. The data indicated that the treatment of MDMs with MANF supplement decreased the proliferation of HCC (Supporting Information Fig. S14A and S14B), suppressed HCC progression (Fig. 8B and C) and tumor neovascularization (Fig. 8D–E), but not affect body weight and the function of liver, kidney and lung (Supporting Information Fig. S15A–S15D). Mechanistically, we found that exogenous His-MANF protein inhibited nuclear import of HSF1 (Fig. S12A), reduced HSP70 protein level (Fig. S12B), reduced M2 maker CD163 expression (Fig. S13A), and up-regulated M1 marker iNOS expression (Fig. S13B). These data suggested that MANF

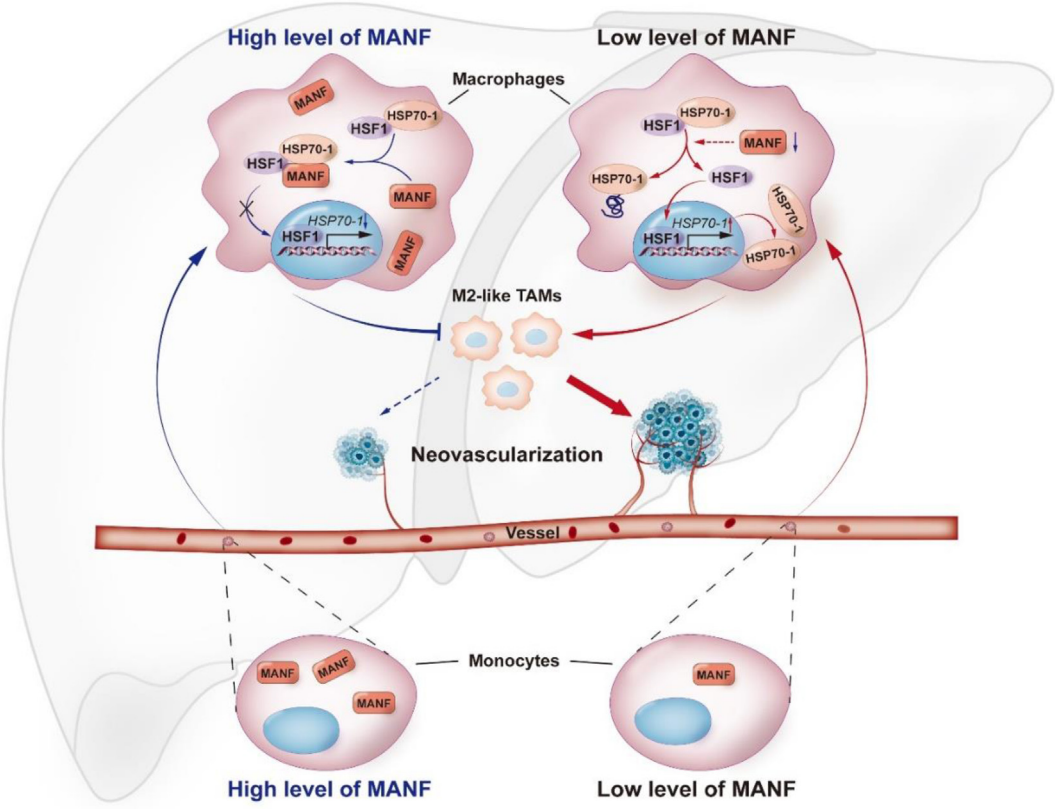


**Figure 9** Schematic diagram.

supplement in MDMs was an effective treatment for HCC through reprogramming TAMs and reducing HCC neovascularization.

## 4. Discussion

In this study, our data indicate that MANF reprograms TAMs into M1 phenotype. Loss of MANF promotes tumor progression of HCC patients and DEN-related mice HCC model, especially tumor neovascularization of HCC. Additionally, our studies to investigate the underlying molecular mechanisms have shown that MANF enhances the HSF1−HSP70-1 interaction, restricts HSF1 in the cytoplasm of macrophages, and decreases both mRNA and protein levels of HSP70-1, which in turn leads to the reprogramming TAMs, reducing the production of pro-angiogenic factors and suppressing neovascularization of HCC.

Hepatic macrophages, the most abundant non-parenchymal cells in the liver, consisted of KCs and MDMs. KCs are the dominant macrophages in healthy livers and play a predominant role in maintaining homeostasis of liver[18]. However, in various injury liver, the number of KCs is rapidly reduced[22,23] along with the recruitment of PBMs to the injured liver area and the differentiation into MDMs[24]. Meanwhile, MDMs, not KCs, are reported to be responsible for the clearance of pre-malignant hepatocytes[25], suggesting that the purpose of monocytes recruitment into liver may be to suppress carcinogenesis. In current study, we found the relatively high MANF level in monocytes/macrophages, and MDMs-derived MANF accounted for a larger proportion of this protein in liver tissues, and it might play an important role in HCC progression. Our previous study verified that hepatocyte-derived MANF is a suppressor of HCC[14]. Thus, hepatocyte-specific knockout mice were used as a control in present study in order to investigate the effect of MDMs-derived MANF on HCC.

In present study, we found hepatic macrophages-derived MANF level was down-regulated in HCC tissues, compared with that in para-cancer tissues. Interestingly, the clinical data also indicated that the level of MANF in PBMs extracted from HCC patients was increased compared to that of healthy volunteer, suggesting that high MANF levels in PBMs of HCC patients may be a compensatory response in the early stage of liver cancer. These data once again indicate that recruitment of MDMs with high level of MANF may increase the level of MANF in the liver tissues to suppress carcinogenesis. However, some HCC patients still had low levels of PBMs-derived MANF, and our RNA-seq data indicated that MANF deficiency did not affect CCR2 level (data not shown in the Figures), an important receptor for monocyte recruitment into liver in MDMs. Therefore, MDMs with both low and high levels of MANF could be recruited into liver cancer tissues. MDMs are accumulated in the new blood vessels of portal vein, where they interact with liver sinusoidal endothelial cells (LSECs)[26] and VEGF is released from MDMs to promote vessel sprouting[27]. Our data indicated MDMs with low MANF levels has a pro-angiogenic feature in HCC.

The vast majority of TAMs exhibit M2-like phenotype, that promote HCC progression, including promoting immunosuppression, neovascularization, the proliferation and metastasis of hepatomas[9]. M2-like TAMs exhibit tumor neovascularization through the production of pro-angiogenic factors, including VEGF, platelet-derived growth factor (PDGF), fibroblast growth factor (FGF), hepatocyte growth factor (HGF), angiostatin, endoglin (CD105), cysteine-rich angiogenic inducer 61 (Cyr61), macrophage-colony stimulating factor 1 (CSF-1)[28-32], VEGF stands out as the main pro-angiogenic factor that promotes endothelial cells proliferation and survival[33,34]. Our data indicating that knockout of MANF resulted in increased levels of several pro-angiogenic factors, such as VEGF, HGF, bFGF and Cyr61 in hepatic macrophages of DEN-treated mice and MDMs cell lines.

Contrary to the pro-tumor effect of M2-like TAMs, M1-like TAMs account for a small proportion and have anti-tumor effects[10]. Since TAMs can switch from one type to another[11], targeting TAMs reprogramming to reduce M2-like phenotype is an important therapy to defeat cancer tissues[12]. In previous study, we found that MANF increased Ly6C$^{low}$ macrophages and subsequently alleviated APAP-induced liver injury[35] and MANF deficiency increased Ly6C$^{high}$ macrophages in $CCl_4$-treated mice model[36], suggesting MANF promoted the transformation of hepatic macrophages into M2 type. We also found that MANF shown the different effects on splenic macrophage differentiation in the healthy (M2 phenotype) and hepatic fibrosis model (M1 phenotype)[37]. In current study, we investigated the function of MANF in TAMs on HCC. These data indicated that MANF increased M1-like phenotype and decreased M2-like phenotype of TAMs *in vitro* and *in vivo*. Furthermore, we verified that MANF supplement in MDMs was an effective therapy for HCC in mice liver orthotopic tumor model.

In order to define the underlying molecular mechanism of MANF-related inhibition of HCC progression (especially TAMs reprogramming and tumor neovascularization), the data observed from IP-MS based proteomics were verified *via* several approaches indicating that MANF interacts with heat shock protein 70-1 (HSP70-1), which is associated with macrophage-mediated neovascularization as the levels of VEGF and HGF were increased in macrophages treated with recombinant HSP70-1 protein[20]. HSP70-1 protein belongs to HSP70 family, and it is an inducible HSP70 protein with low level in normal cells[38]. When cells are stressed, the level of HSP70-1 is increased rapidly[38]. There are several studies reporting that inducible HSP70 (HSP70-1) promotes neovascularization and HCC progression. Firstly, the levels of HSP70 proteins are increased both in the tumor tissues and in the blood of HCC patients compared to heathy volunteers[39,40]. Secondly, HSP70 is a sensitive biomarker for the diagnosis of early HCC[41], and high level of HSP70 predicts poor prognosis of HCC patients[42]. Lastly, the knockout of HSP70-1 decreases neovascularization and suppresses tumorigenesis of HCC mice[43]. HSP70-1 is not only derived from hepatocytes, but also localized in hepatic macrophages, particularly MDMs[44]. We also verified macrophages overexpressing HSP70-1 exhibited M2-like phenotype. In present study, we detected *HSP70-1* mRNA level, but only total HSP70 proteins were detected because of lack of HSP70-1 antibody. Since the increase of HSP70 protein is inducible HSP70 protein (HSP70-1) in HCC, detection of total HSP70 protein level in current study is also reasonable.

Upregulation of VEGF and HGF levels in macrophages treated with recombinant HSP70-1 protein reflects its role in macrophage-mediated neovascularization[45]. Concomitantly, our data indicated that MDMs-derived MANF inhibited the level of HSP70-1 as well

as decreased VEGF and HGF levels. VEGF and HGF proteins derived from MDMs not only promote neovascularization of HCC, but also may increase the proliferation of hepatocytes. Although VEGF does not mediate the proliferation of hepatocytes *in vitro*, data from *in vivo* studies or co-culture of hepatocytes with endothelial cells have shown that VEGF promotes hepatocyte proliferation through VEGF−VEGFR pathway[46]. Furthermore, HGF stimulate the proliferation of hepatocytes through HGF/c-Met pathway[47,48]. Thus, the mechanism underlying the stimulation of hepatocytes proliferation and suppression of apoptosis may be increased levels MDMs-derived VEGF and HGF proteins, which also promotes tumor neovascularization.

## 5. Conclusions

Taken together, our data indicate that MANF enhances the interaction of HSF1 and HSP70-1, which in turn inhibits the nuclear translocation of HSF1 and the transcription of HSP70-1 in hepatic macrophages, leads to the reprogramming of TAMs, inhibiting of tumor neovascularization and HCC progression (Fig. 9). Our study contributes to the exploration the mechanism of TAMs reprogramming and MDMs-mediated tumor neovascularization, which may provide insights for future therapeutic exploitation of HCC.

## Acknowledgments

This work was funded by support programs for Jun Liu, including the National Natural Science Foundation of China (82073862), Excellent Youth Talent Program of Anhui Province Natural Science Foundation (2108085Y27, China). This work was also funded by Anhui Province Natural Science Foundation (2208085MH284, China) for Xiangpeng Hu, and funded by the National Natural Science Foundation of China (U21A20345) for Yuxian Shen. We express our gratitude to Prof. Haiming Wei (University of Science and Technology of China) for his guidance. We also thank Dr. Jia Luo (University of Kentucky, USA) for supplying *MANF*$^{flox/flox}$ mice.

## Author contributions

Dan Han: Investigation. Qiannan Ma: Investigation. Petek Ballar: Writing − review & editing. Chunyang Zhang: Investigation. Min Dai: Investigation. Xiaoyuan Luo: Investigation. Jiong Gu: Investigation. Chuansheng Wei: Investigation. Panhui Guo: Investigation. Lulu Zeng: Investigation. Min Hu: Investigation. Can Jiang: Investigation. Yanyan Liang: Investigation. Yanyan Wang: Investigation. Chao Hou: Investigation. Xian Wang: Investigation. Lijie Feng: Supervision. Yujun Shen: Investigation. Yuxian Shen: Conceptualization, Funding acquisition. Xiangpeng Hu: Conceptualization, Investigation. Jun Liu: Conceptualization, Funding acquisition, Writing − original draft, Writing − review & editing.

## Conflicts of interest

The authors declare no potential conflicts of interest.

## Appendix A. Supporting information

Supporting information to this article can be found online at https://doi.org/10.1016/j.apsb.2024.05.001.

## References

1. Villanueva A. Hepatocellular carcinoma. *N Engl J Med* 2019;**380**:1450−62.
2. Kim E, Viatour P. Hepatocellular carcinoma: old friends and new tricks. *Exp Mol Med* 2020;**52**:1898−907.
3. Llovet JM, Kelley RK, Villanueva A, Singal AG, Pikarsky E, Roayaie S, et al. Hepatocellular carcinoma. *Nat Rev Dis Prim* 2021;**7**:6.
4. Chen S, Cao Q, Wen W, Wang H. Targeted therapy for hepatocellular carcinoma: challenges and opportunities. *Cancer Lett* 2019;**460**:1−9.
5. Afra F, Mahboobipour AA, Salehi Farid A, Ala M. Recent progress in the immunotherapy of hepatocellular carcinoma: non-coding rna-based immunotherapy may improve the outcome. *Biomed Pharmacother* 2023;**165**:115104.
6. Sangro B, Sarobe P, Hervas-Stubbs S, Melero I. Advances in immunotherapy for hepatocellular carcinoma. *Nat Rev Gastroenterol Hepatol* 2021;**18**:525−43.
7. Tang W, Chen Z, Zhang W, Cheng Y, Zhang B, Wu F, et al. The mechanisms of sorafenib resistance in hepatocellular carcinoma: theoretical basis and therapeutic aspects. *Signal Transduct Targeted Ther* 2020;**5**:87.
8. Yuen VW, Wong CC. Hypoxia-inducible factors and innate immunity in liver cancer. *J Clin Invest* 2020;**130**:5052−62.
9. Zheng H, Peng X, Yang S, Li X, Huang M, Wei S, et al. Targeting tumor-associated macrophages in hepatocellular carcinoma: biology, strategy, and immunotherapy. *Cell Death Dis* 2023;**9**:65.
10. Yang Q, Guo N, Zhou Y, Chen J, Wei Q, Han M. The role of tumor-associated macrophages (tams) in tumor progression and relevant advance in targeted therapy. *Acta Pharm Sin B* 2020;**10**:2156−70.
11. Vitale I, Manic G, Coussens LM, Kroemer G, Galluzzi L. Macrophages and metabolism in the tumor microenvironment. *Cell Metabol* 2019;**30**:36−50.
12. Zhang X, Li S, Malik I, Do MH, Ji L, Chou C, et al. Reprogramming tumour-associated macrophages to outcompete cancer cells. *Nature* 2023;**619**:616−23.
13. Broutier L, Andersson-Rolf A, Hindley CJ, Boj SF, Clevers H, Koo BK, et al. Culture and establishment of self-renewing human and mouse adult liver and pancreas 3d organoids and their genetic manipulation. *Nat Protoc* 2016;**11**:1724−43.
14. Liu J, Wu Z, Han D, Wei C, Liang Y, Jiang T, et al. Mesencephalic astrocyte-derived neurotrophic factor inhibits liver cancer through small ubiquitin-related modifier (SUMO)ylation-related suppression of NF-kappaB/snail signaling pathway and epithelial-mesenchymal transition. *Hepatology* 2020;**71**:1262−78.
15. Hu X, Han D, Wang Y, Gu J, Wang X, Jiang Y, et al. Phospho-smad3l promotes progression of hepatocellular carcinoma through decreasing mir-140-5p level and stimulating epithelial−mesenchymal transition. *Dig Liver Dis* 2021;**53**:1343−51.
16. Wei R, Zhu WW, Yu GY, Wang X, Gao C, Zhou X, et al. S100 calcium-binding protein A9 from tumor-associated macrophage enhances cancer stem cell-like properties of hepatocellular carcinoma. *Int J Cancer* 2021;**148**:1233−44.
17. Sharma A, Seow JJW, Dutertre CA, Pai R, Bleriot C, Mishra A, et al. Onco-fetal reprogramming of endothelial cells drives immunosuppressive macrophages in hepatocellular carcinoma. *Cell* 2020;**183**:377.
18. Wen Y, Lambrecht J, Ju C, Tacke F. Hepatic macrophages in liver homeostasis and diseases-diversity, plasticity and therapeutic opportunities. *Cell Mol Immunol* 2021;**18**:45−56.
19. Xu HY, Jiao YH, Li SY, Zhu X, Wang S, Zhang YY, et al. Hepatocyte-derived manf mitigates ethanol-induced liver steatosis in mice *via* enhancing ass1 activity and activating ampk pathway. *Acta Pharmacol Sin* 2023;**44**:157−68.
20. Kim TK, Na HJ, Lee WR, Jeoung MH, Lee S. Heat shock protein 70-1a is a novel angiogenic regulator. *Biochem Biophys Res Commun* 2016;**469**:222−8.

21. Pincus D. Regulation of Hsf1 and the heat shock response. *Adv Exp Med Biol* 2020;**1243**:41−50.
22. Borst K, Frenz T, Spanier J, Tegtmeyer PK, Chhatbar C, Skerra J, et al. Type I interferon receptor signaling delays kupffer cell replenishment during acute fulminant viral hepatitis. *J Hepatol* 2018;**68**:682−90.
23. Bleriot C, Dupuis T, Jouvion G, Eberl G, Disson O, Lecuit M. Liver-resident macrophage necroptosis orchestrates type 1 microbicidal inflammation and type-2-mediated tissue repair during bacterial infection. *Immunity* 2015;**42**:145−58.
24. Beattie L, Sawtell A, Mann J, Frame TCM, Teal B, de Labastida Rivera F, et al. Bone marrow-derived and resident liver macrophages display unique transcriptomic signatures but similar biological functions. *J Hepatol* 2016;**65**:758−68.
25. Lahmar Q, Keirsse J, Laoui D, Movahedi K, Van Overmeire E, Van Ginderachter JA. Tissue-resident versus monocyte-derived macrophages in the tumor microenvironment. *Biochim Biophys Acta* 2016;**1865**:23−34.
26. Ehling J, Bartneck M, Wei X, Gremse F, Fech V, Mockel D, et al. Ccl2-dependent infiltrating macrophages promote angiogenesis in progressive liver fibrosis. *Gut* 2014;**63**:1960−71.
27. Corliss BA, Azimi MS, Munson JM, Peirce SM, Murfee WL. Macrophages: an inflammatory link between angiogenesis and lymphangiogenesis. *Microcirculation* 2016;**23**:95−121.
28. Morse MA, Sun W, Kim R, He AR, Abada PB, Mynderse M, et al. The role of angiogenesis in hepatocellular carcinoma. *Clin Cancer Res* 2019;**25**:912−20.
29. Joo YY, Jang JW, Lee SW, Yoo SH, Kwon JH, Nam SW, et al. Circulating pro- and anti-angiogenic factors in multi-stage liver disease and hepatocellular carcinoma progression. *Sci Rep* 2019;**9**:9137.
30. Babic AM, Kireeva ML, Kolesnikova TV, Lau LF. Cyr61, a product of a growth factor-inducible immediate early gene, promotes angiogenesis and tumor growth. *Proc Natl Acad Sci U S A* 1998;**95**:6355−60.
31. Fagiani E, Christofori G. Angiopoietins in angiogenesis. *Cancer Lett* 2013;**328**:18−26.
32. Laoui D, Van Overmeire E, De Baetselier P, Van Ginderachter JA, Raes G. Functional relationship between tumor-associated macrophages and macrophage colony-stimulating factor as contributors to cancer progression. *Front Immunol* 2014;**5**:489.
33. Binet F, Sapieha P. Er stress and angiogenesis. *Cell Metabol* 2015;**22**:560−75.
34. Wu SX, Ye SS, Hong YX, Chen Y, Wang B, Lin XJ, et al. Hepatitis B virus small envelope protein promotes hepatocellular carcinoma angiogenesis *via* endoplasmic reticulum stress signaling to upregulate the expression of vascular endothelial growth factor A. *J Virol* 2022;**96**:e0197521.
35. Hou X, Liu Q, Gao Y, Yong L, Xie H, Li W, et al. Mesencephalic astrocyte-derived neurotrophic factor reprograms macrophages to ameliorate acetaminophen-induced acute liver injury *via* p38 mapk pathway. *Cell Death Dis* 2022;**13**:100.
36. Hou C, Wang D, Zhao M, Ballar P, Zhang X, Mei Q, et al. Manf brakes tlr4 signaling by competitively binding s100a8 with s100a9 to regulate macrophage phenotypes in hepatic fibrosis. *Acta Pharm Sin B* 2023;**13**:4234−52.
37. Hou C, Wang D, Li X, He Y, Wei C, Jiang R, et al. Manf regulates splenic macrophage differentiation in mice. *Immunol Lett* 2019;**212**:37−45.
38. Wu J, Liu T, Rios Z, Mei Q, Lin X, Cao S. Heat shock proteins and cancer. *Trends Pharmacol Sci* 2017;**38**:226−56.
39. Joo M, Chi JG, Lee H. Expressions of hsp70 and hsp27 in hepatocellular carcinoma. *J Kor Med Sci* 2005;**20**:829−34.
40. Gehrmann M, Cervello M, Montalto G, Cappello F, Gulino A, Knape C, et al. Heat shock protein 70 serum levels differ significantly in patients with chronic hepatitis, liver cirrhosis, and hepatocellular carcinoma. *Front Immunol* 2014;**5**:307.
41. Chuma M, Sakamoto M, Yamazaki K, Ohta T, Ohki M, Asaka M, et al. Expression profiling in multistage hepatocarcinogenesis: identification of hsp70 as a molecular marker of early hepatocellular carcinoma. *Hepatology* 2003;**37**:198−207.
42. Wang B, Lan T, Xiao H, Chen ZH, Wei C, Chen LF, et al. The expression profiles and prognostic values of HSP70s in hepatocellular carcinoma. *Cancer Cell Int* 2021;**21**:286.
43. Cho W, Jin X, Pang J, Wang Y, Mivechi NF, Moskophidis D. The molecular chaperone heat shock protein 70 controls liver cancer initiation and progression by regulating adaptive DNA damage and mitogen-activated protein kinase/extracellular signal-regulated kinase signaling pathways. *Mol Cell Biol* 2019;**39**:e00391.18.
44. Martine P, Chevriaux A, Derangere V, Apetoh L, Garrido C, Ghiringhelli F, et al. Hsp70 is a negative regulator of NLRP3 inflammasome activation. *Cell Death Dis* 2019;**10**:256.
45. Khan KN, Kitajima M, Imamura T, Hiraki K, Fujishita A, Sekine I, et al. Toll-like receptor 4-mediated growth of endometriosis by human heat-shock protein 70. *Hum Reprod* 2008;**23**:2210−9.
46. DeLeve LD. Liver sinusoidal endothelial cells and liver regeneration. *J Clin Invest* 2013;**123**:1861−6.
47. Bradley CA, Salto-Tellez M, Laurent-Puig P, Bardelli A, Rolfo C, Tabernero J, et al. Targeting c-met in gastrointestinal tumours: rationale, opportunities and challenges. *Nat Rev Clin Oncol* 2017;**14**:562−76.
48. Bozkaya G, Korhan P, Cokakli M, Erdal E, Sagol O, Karademir S, et al. Cooperative interaction of muc1 with the HGF/c-met pathway during hepatocarcinogenesis. *Mol Cancer* 2012;**11**:64.